



Published in final edited form as:

Urology. 2020 May ; 139: 134–140. doi:10.1016/j.urology.2019.01.008.

Ex-vivo Imaging of Upper Tract Urothelial Carcinoma Using Novel pH Low Insertion Peptide (Variant 3), a Molecular Imaging Probe

Joseph Brito, Borivoj Golijanin, Ohad Kott, Anna Moshnikova, Catrina Mueller-Leonhard, Boris Gershman, Oleg A. Andreev, Yana K. Reshetnyak, Ali Amin, Dragan Golijanin
Urology Department, Yale University School of Medicine, New Haven, CT; the Department of Pathology & Laboratory Medicine, The Warren Alpert Medical School of Brown University and The Miriam Hospital, Providence, RI; the Urology Department, Minimally Invasive Urology Institute, Warren Alpert Medical School of Brown University and The Miriam Hospital, Providence, RI; and the Physics Department, University of Rhode Island, Kingston, RI

Abstract

OBJECTIVE—To improve visualization of upper tract urothelial carcinomas. Previous studies using the novel pH low insertion peptide (pHLIP) variant 3 (Var3) conjugated to indocyanine green (ICG) have demonstrated high sensitivity and specificity for imaging of bladder urothelial carcinoma. Here, we describe a novel approach for the imaging of upper tract urothelial carcinomas using ICG-Var3 pHLIP.

METHODS—Twelve ex-vivo upper urinary tract specimens were irrigated with ICG-Var 3 pHLIP for 15 minutes and then examined using a white light laparoscopic camera followed by near infrared fluorescent (NIRF) imaging using a Stryker 1588 AIM imaging system. Standard histopathologic evaluation was performed and findings were correlated with white light and ICG-Var3 NIRF imaging. One patient who underwent radical nephrectomy for renal cell carcinoma was used as a negative control.

RESULTS—Nineteen lesions were identified on histopathologic evaluation in 10 patients, including 82% high-grade urothelial carcinoma and 18% low-grade urothelial carcinoma. Nineteen (100%) malignant lesions were identified using NIRF imaging, while 15 (78.9%) lesions were identified using conventional white light examination. The sensitivity of ICG-Var3 pHLIP NIRF imaging was 100% compared to 78.9% white light examination. Both modalities are 100% specific. Benign collecting systems and ureters did not show uptake of the pHLIP construct.

CONCLUSION—In this feasibility study, the ICG-Var3 pHLIP imaging agent demonstrated superior diagnostic performance compared to conventional white light examination. While additional studies are required for validation and in-vivo translation, pHLIP-based imaging

Address correspondence to: Dragan Golijanin, M.D., Urology Department, Minimally Invasive Urology Institute, Warren Alpert Medical School of Brown University and The Miriam Hospital, 164 Summit Street, Providence, RI 02906. Dragan.Golijanin@lifespan.org.

SUPPLEMENTARY MATERIALS

Supplementary material associated with this article can be found in the online version at <https://doi.org/10.1016/j.urology.2019.01.008>.

represents a promising tool to improve the evaluation and management of upper tract urothelial carcinoma. *UROLOGY* 139: 134–140, 2020.

Upper tract urothelial cell carcinoma (UTUC) accounts for 5%–10% of all urothelial neoplasms and has increased in incidence over the last 4 decades.^{1,2} Although, enhanced cystoscopic techniques have become increasingly adopted for the endoscopic diagnosis and management of lower tract urothelial carcinoma,^{3–5} there are limited data for the use of such approaches in upper tract urothelial carcinoma.^{6–11}

The pH low insertion peptides (pHLIP) belong to a family of water soluble membrane peptides that have been shown to target the acidic microenvironment of malignant cells based on the Warburg effect.¹² pHLIPs target low pH at the surface of cancer cells, where it is the lowest and independent of tumor perfusion, thus providing high specificity and sensitivity in tumor targeting.¹³ In preclinical trials, pHLIP has been used for imaging and pH specific drug delivery.^{14–21} Among investigated pHLIPs variant 3 (Var3) demonstrated the best tumor targeting.^{14,19,20} Currently ¹⁸F-Var3 pHLIP is underway to clinical translation for imaging of acidity.²⁰ In a previous study using ICG-Var3 pHLIP, we demonstrated targeting of bladder urothelial carcinoma with high sensitivity (97%) and specificity (100%).²¹ Here, we report on a feasibility study for the use of ICG-Var3 pHLIP-based imaging of upper tract urothelial carcinoma in *ex-vivo* specimens.

MATERIALS AND METHODS

Study Cohort

Following Institutional Review Board approval, 12 consecutive patients undergoing surgical treatment of upper urinary tract malignancy ($N=11$ UTUC; $N=1$ RCC) at the Miriam Hospital (Providence, RI) were prospectively enrolled and consented for participation in this study. All surgeries were performed by a single urologic oncologist (D.G.).

Specimen Processing and Imaging Evaluation

ICG-Var3 was prepared as described previously.¹⁵ For each case, 100 mL of solution containing 0.40 μ mol of ICG-Var3 in Phosphate Buffered Saline (PBS), pH 7.4, supplemented with 10 mM D-glucose was freshly prepared. After excision of the upper urinary tract specimen, an open-ended ureteral catheter was inserted into the ureter. Samples were washed with 100 mL of normal saline for 15 minutes. Upper tracts were then slowly irrigated with the freshly prepared 100 mL of ICG-Var3 pHLIP solution for 15 minutes, followed by another wash with 100 mL of normal saline. The washed upper tract specimens were incised longitudinally. Ex-vivo evaluation of the upper urinary tracts was performed using Stryker 1588 AIM imaging system using 10 mm and 5 mm laparoscopes under white light followed by near infrared fluorescent (NIRF) imaging by a single investigator trained in NIRF imaging (B.G.). White light examination preceded NIRF imaging in every case. In 2 cases the DaVinci Si Surgical System Firefly (Intuitive Surgical, Sunnyvale, CA) was used. Areas labeled by ICG-Var3 pHLIP were marked by ink and entirely submitted for standard histopathologic evaluation by a single genitourinary pathologist (A.A.).

Histopathologic Evaluation

Following imaging, specimens were sectioned and submitted after 24-hour fixation in 10% phosphate-buffered formalin according to the standard institutional grossing manual. Samples were processed for routine histology into paraffin embedded blocks. Five micrometer thick tissue sections were obtained and stained for Hematoxylin & Eosin (H&E). Evaluation of pathology was performed by a genitourinary pathologist and a standard report was prepared based on the American Joint Committee on Cancer Staging Manual, seventh edition, 2010. Correlation between presence of ICG-Var3 NIRF stained lesions, standard gross white light evaluation, and routine histopathologic evaluation was assessed.

Statistical Analysis

Clinicopathologic features were summarized in frequency tables. Fisher's Exact chi-square analysis was used to correlate the difference between white light and NIRF to presence of malignancy. Statistical analyses were performed using IBM SPSS Statistics for Windows Version 20 (IBM (IBM Corp, Armonk, NY), with *P* values <.05 considered statistically significant.

RESULTS

Twelve patients were included in the study, of whom 11 underwent radical nephroureterectomy (*N*= 10) or distal ureterectomy (*N*= 1) for UTUC, while 1 control patient underwent radical nephrectomy for Renal Cell Carcinoma (RCC) (Table 1, Supplementary Table 1a). A total of 19 urothelial carcinoma lesions were identified by standard histopathologic evaluation, including 8 (42.1%) invasive UTUC and 11 (57.9%) noninvasive UTUC (Table 1, Supplementary Table 1b). Fifteen (78.9%) lesions were high-grade and 4 (21.1%) were low-grade.

ICG-Var3 NIRF ex-vivo imaging identified 19 lesions, while conventional white light examination identified 15 lesions (Table 2a and 2b).

Figure 1 demonstrates representative images of ICG-Var3 pHLIP targeting of high-grade invasive (Fig. 1A–C), high-grade noninvasive (Fig. 1D–F), and low-grade noninvasive (Fig. 1G–I) lesions. Three lesions were low-grade noninvasive UTUC. Of the 9 invasive high-grade lesions, 2 were presented with features of small cell carcinoma, and 1 with squamous differentiation.

Compared to white light examination, NIRF pHLIP-based imaging demonstrated superior sensitivity in visualizing UTUC (100% vs 78.9%; *P*= .001) and equal specificity (100% vs 100%) (Table 3).

Without the aid of ICG-Var3 pHLIP (white light assessment only), only 15 lesions were grossly identified (78.9%). Of the lesions missed by white light assessment, 3 were high-grade noninvasive papillary UCC, and the fourth missed lesion was low-grade noninvasive UCC

In all cases, routine histopathologic evaluation demonstrated that benign urothelium, ureter, and the renal pelvis did not show any uptake of the pHLIP construct. Nonmalignant lesions like ureteritis cystica (6 locations) seen in the control patient were negative for ICG-Var3 pHLIP staining (Fig. 1J–L).

DISCUSSION

In this feasibility study, the ICG-Var3 pHLIP NIRF imaging agent demonstrated excellent performance for the diagnosis of upper tract urothelial carcinoma, with 100% specificity and sensitivity. It improved the diagnosis of UTUC by 21.2% compared to conventional white light examination, identifying lesions not seen using white light gross examination due to small size. Normal mucosa was not stained by ICG-Var3 pHLIP, nor were nonmalignant lesions such as ureteritis cystica.

Cross-sectional imaging and traditional white-light endoscopic visual have historically demonstrated poor performance for the diagnosis and staging of UTUC.^{22–24} Recognizing the need for better and more accurate diagnostic methods, new technologies have been proposed. Maruschke et al detailed various imaging techniques used for UTUC identification in a retrospective cohort of 113 patients, citing sensitivities of 87.7% for retrograde ureteropyelography, 83.1% for CT scan, 57.4% for intravenous urograms, and 50% for MRI.²⁵ Although prior studies have reported on the performance of diagnostic imaging modalities such as computed tomography, intravenous urograms, and magnetic resonance imaging, none of these imaging modalities are a substitute for the direct visualization of tumors that is required to perform endoscopic biopsy.

Novel and advanced ureteroscopic techniques are extensively reported in a review by Baard et al in which benefits of narrow band imaging (NBI), Image 1S, and photodynamic diagnosis (PDD) for augmenting ureteroscopy (URS), especially as aids in diagnosing carcinoma in Situ and sessile lesions that may otherwise be difficult to identify.⁷ Advances in augmented and enhanced URS are further reviewed by Knoedler and Raman, describing the few reported cases where NBI was used with great success, the high specificity of PDD and difficulties associated with administration of the necessary fluorochrome, and the emerging confocal imaging microscopy of UTUC.²⁶ Nonetheless, novel imaging modalities for the diagnosis of UTUC require more study as pitfalls have been documented. NBI provides subjective improvements in the visualization, with few noticeable improvements in the image compared to white light URS²⁷; the fluorochrome associated with PDD can have adverse effects in up to 25.8% of patients¹⁰; and confocal imaging microscopy has been reported with unreliable relationship to tumor grade and stage.²⁸ Utility of these advanced imaging modalities in diagnosis and management of UTUC is unmistakable, as white light URS has been reported as falsely omitting up to 50% of lesions in patients undergoing URS for UTUC and up to 15% of high-grade lesions are misdiagnosed as low-grade.^{29,30}

This is the first study to report the feasibility of enhanced visual diagnosis of upper tract urothelial carcinoma using a novel and specific targeting agent, as has become accepted for lower tract urothelial carcinoma.²¹ The pHLIP peptide is specific to cellular microenvironments with higher acidity, with high rates of glucose metabolism, and can

detect 0.2–0.3 pH unit changes in vivo.^{13,14} Additionally, the ICG-Var3 pHLIP signal is easier to make out than that in NBI and PDD. In this regard, the pHLIP construct holds great promise to improve the evaluation and management of UTUC.

Since histopathologic diagnosis of UTUC is based on endoscopic identification of tumors, it follows that improved diagnostic tools will enhance current techniques. To this end, NIRF pHLIP-based imaging may facilitate endoscopic identification of target lesion or biopsy and treatment. pHLIP based targeting may have other applications in the management of UTUC-including enhancing the performance of urine cytologic evaluation, targeting lesions for endoscopic ablation, or allowing novel drug delivery mechanisms of pHLIP to be implemented in targeted treatments of urothelial carcinomas. However, these applications require further research.

This study has a number of limitations. First and fore-most, it is a small, ex-vivo feasibility study; as such, results will need to be validated in larger cohorts, and more importantly, translated into in-vivo applications. This will require validation of NIRF-based imaging within ureteroscopic approaches to determine whether smaller scope diameter, tangential lesion viewing, and in-vivo irrigation limit lesion identification. In addition, the ability of pHLIP-based imaging to enhance staging and differentiation of low-grade vs high-grade lesions is a critical question of clinical importance. Finally, we compared NIRF imaging to conventional white light evaluation; although white light ureteroscopic examination remains the standard of care in the diagnosis of UTUC, the recent adoption of enhanced cystoscopic techniques, such as PDD and NBI, will require comparison with pHLIP if they are adapted for upper tract use. Despite these limitations, pHLIP-based NIRF imaging demonstrated very encouraging results for the identification of UTUC that require validation in ongoing studies.

Supplementary Material

Refer to Web version on PubMed Central for supplementary material.

Acknowledgment.

The authors are grateful to their partner, Stryker Endoscopy (San Jose, CA), for providing imaging system and technical assistance. The research reported in this publication was supported in part by the National Institute of General Medical Sciences of the National Institutes of Health under award number R01GM073857 to O.A.A. and Y.K.R., and in part by the Feibelman Family research grant awarded to DG.

Financial Disclosure:

O.A.A. and Y.K.R. are founders of pHLIP, Inc. They have shares in the company, but the company did not fund any part of the work reported in the paper, which was done in their academic laboratories.

References

1. Soria F, Shariat SF, Lerner SP, et al. Epidemiology, diagnosis, preoperative evaluation and prognostic assessment of upper-tract urothelial carcinoma (UTUC). *World J Urol.* 2017;35:379–387. [PubMed: 27604375]
2. Raman JD, Messer J, Sielatycki JA, Hollenbeak CS. Incidence and survival of patients with carcinoma of the ureter and renal pelvis in the USA, 1973–2005. *BJU Int.* 2011;107:1059–1064. [PubMed: 20825397]

3. Babjuk M, Böhle A, Burger M, et al. EAU Guidelines on Non–Muscle-invasive Urothelial Carcinoma of the Bladder: Update 2016. *Eur Urol.* 2017;71:447–461. [PubMed: 27324428]
4. Chang SS, Boorjian SA, Chou R, et al. Diagnosis and treatment of non-muscle invasive bladder cancer: AUA/SUO guideline. *J Urol.* 2016;196:1021–1029. [PubMed: 27317986]
5. Spiess PE, Agarwal N, Bangs R, et al. Bladder cancer, version 5.2017, NCCN clinical practice guidelines in oncology. *J Natl Compr Canc Netw.* 2017;15:1240–1267. [PubMed: 28982750]
6. Aragon-Ching JB. Challenges and advances in the diagnosis, biology, and treatment of urothelial upper tract and bladder carcinomas. *Urol Oncol.* 2017;35:462–464. [PubMed: 28625477]
7. Baard J, Freund JE, de la Rosette JJ, Laguna MP. New technologies for upper tract urothelial carcinoma management. *Curr Opin Urol.* 2017;27:170–175. [PubMed: 28085698]
8. Kata SG, Aboumarzouk OM, Zreik A, et al. Photodynamic diagnostic ureterorenoscopy: a valuable tool in the detection of upper urinary tract tumour. *Photodiagnosis Photodyn Ther.* 2016;13:255–260. [PubMed: 26256824]
9. Mathieu R, Bensalah K, Lucca I, et al. Upper urinary tract disease: what we know today and unmet needs. *Transl Androl Urol.* 2015;4:261–272. [PubMed: 26816829]
10. Osman E, Alnaib Z, Kumar N. Photodynamic diagnosis in upper urinary tract urothelial carcinoma: a systematic review. *Arab J Urol.* 2017;15:100–109. [PubMed: 29071138]
11. Wetherell DR, Ling D, Ow D, et al. Advances in ureteroscopy. *Transl Androl Urol.* 2014;3:321–327. [PubMed: 26816786]
12. Wyatt LC, Lewis JS, Andreev OA, Reshetnyak YK, Engelman DM. Applications of pHLIP technology for cancer imaging and therapy. *Trends biotechnol.* 2017;35:653–664. [PubMed: 28438340]
13. Anderson M, Moshnikova A, Engelman DM, Reshetnyak YK, Andreev OA. Probe for the measurement of cell surface pH in vivo and ex vivo. *Proc Natl Acad Sci U S A.* 2016;113:8177–8181. [PubMed: 27382181]
14. Adochite RC, Moshnikova A, Golijanin J, et al. Comparative study of tumor targeting and biodistribution of pH (Low) insertion peptides (pHLIP((R)) Peptides) conjugated with different fluorescent dyes. *Mol Imaging Biol.* 2016;18:686–696. [PubMed: 27074841]
15. Cheng CJ, Bahal R, Babar IA, et al. MicroRNA silencing for cancer therapy targeted to the tumour microenvironment. *Nature.* 2015;518:107–110. [PubMed: 25409146]
16. Ozes AR, Wang Y, Zong X, et al. Therapeutic targeting using tumor specific peptides inhibits long non-coding RNA HOTAIR activity in ovarian and breast cancer. *Sci Rep.* 2017;7:894. [PubMed: 28420874]
17. Tapmeier TT, Moshnikova A, Beech J, et al. The pH low insertion peptide pHLIP Variant 3 as a novel marker of acidic malignant lesions. *Proc Natl Acad Sci U S A.* 2015;112:9710–9715. [PubMed: 26195776]
18. Wei Y, Liao R, Mahmood AA, Xu H, Zhou Q. pH-responsive pHLIP (pH low insertion peptide) nanoclusters of superparamagnetic iron oxide nanoparticles as a tumor- selective MRI contrast agent. *Acta Biomater.* 2017;55:194–203. [PubMed: 28363789]
19. Wyatt LC, Moshnikova A, Crawford T, Engelman DM, Andreev OA, Reshetnyak YK. Peptides of pHLIP family for targeted intracellular and extracellular delivery of cargo molecules to tumors. *Proc Natl Acad Sci U S A.* 2018;115:E2811–E2818. [PubMed: 29507241]
20. Demoin DW, Wyatt LC, Edwards KJ, et al. PET imaging of extracellular pH in tumors with (64)Cu- and (18)F-labeled pHLIP peptides: a structure-activity optimization study. *Bioconjug Chem.* 2016;27:2014–2023. [PubMed: 27396694]
21. Golijanin J, Amin A, Moshnikova A, et al. Targeted imaging of urothelium carcinoma in human bladders by an ICG pHLIP peptide ex vivo. *Proc Natl Acad Sci U S A.* 2016;113:11829–11834. [PubMed: 27688767]
22. Grahn A, Melle-Hannah M, Malm C, et al. Diagnostic accuracy of computed tomography urography and visual assessment during ureterorenoscopy in upper tract urothelial carcinoma. *BJU Int.* 2017;119:289–297. [PubMed: 27611622]
23. Jeon SS, Sung HH, Jeon HG, et al. Endoscopic management of upper tract urothelial carcinoma: improved prediction of invasive cancer using a ureteroscopic scoring model. *Surg Oncol.* 2017;26:252–256. [PubMed: 28807244]

24. Mammen S, Krishna S, Quon M, et al. Diagnostic accuracy of qualitative and quantitative computed tomography analysis for diagnosis of pathological grade and stage in upper tract urothelial cell carcinoma. *J Comput Assist Tomogr.* 2018;42:204–210. [PubMed: 28937484]
25. Maruschke M, Kram W, Zimpfer A, Kundt G, Hakenberg OW. Upper urinary tract tumors: which diagnostic methods are needed. *Urol Int.* 2017;98:304–311. [PubMed: 28241123]
26. Knoedler JJ, Raman JD. Advances in the management of upper tract urothelial carcinoma: improved endoscopic management through better diagnostics. *Ther Adv Urol.* 2018;10:421–429. [PubMed: 30574202]
27. Traxer O, Geavlete B, de Medina SG, Sibony M, Al-Qahtani SM. Narrow-band imaging digital flexible ureteroscopy in detection of upper urinary tract transitional-cell carcinoma: initial experience. *J Endourol.* 2011;25:19–23. [PubMed: 21247287]
28. Breda A, Territo A, Guttilla A, et al. Correlation between confocal laser endomicroscopy (Cellvizio((R))) and histological grading of upper tract urothelial carcinoma: a step forward for a better selection of patients suitable for conservative management. *Eur Urol Focus.* 2018;4:954–959. [PubMed: 28753800]
29. Yamany T, van Batavia J, Ahn J, Shapiro E, Gupta M. Ureterorenoscopy for upper tract urothelial carcinoma: how often are we missing lesions. *Urology.* 2015;85:311–315. [PubMed: 25623674]
30. Straub J, Strittmatter F, Karl A, Stief CG, Tritschler S. Ureterorenoscopic biopsy and urinary cytology according to the 2004 WHO classification underestimate tumor grading in upper urinary tract urothelial carcinoma. *Urol Oncol.* 2013;31:1166–1170. [PubMed: 22300757]

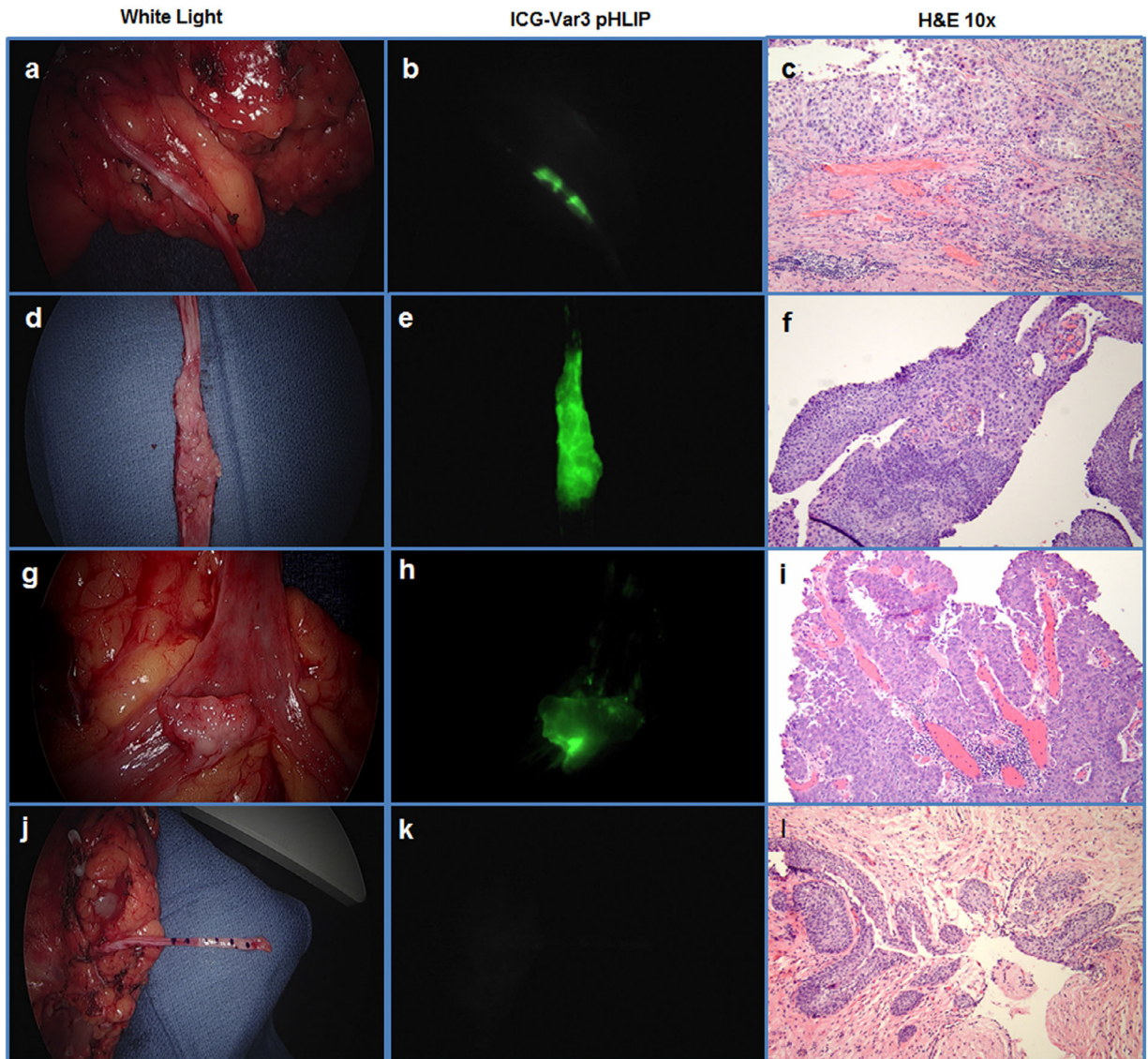


Figure 1. Ex vivo human upper tract urothelial carcinoma. (A-C) Case #5, high-grade UTUC, pT3NxMx; (D-F) case #9, high-grade noninvasive papillary UTUC, pTaN0Mx; (G-I) case # 8, noninvasive low-grade UTUC, pTaNxMx; (J-L) case #6, control—no tumor seen in ureteritis cystica. White light (A, D, G, J), ICG-Var3 NIRF (B, E, H, K), and (H) and (E) (C, F, I, L) images are presented.

Table 1. Demographic and pathology of lesions in 10 cases examined by white light and ICG-Var3 pHLIP NIRF imaging

Case	Sex/Age (y)	Pathologic Stage	Pathologic Diagnosis	Grade	Location	Depth	Size	Lesion Number	White Light Diagnosis	NIRF Imaging
1	F/67	pT1NxMx	Invasive high-grade papillary urothelial carcinoma	HGI	Proximal ureter	Lamina propria	4.2 cm	1	+	+
2	M/68	pT2NxMx	Invasive high-grade papillary urothelial carcinoma	HGI						
			Ureteropelvic junction		Muscularis propria	3.0 cm	2	+	+	
3	F/75	mpTa	Noninvasive high-grade papillary urothelial carcinoma	HGN	Distal ureter and bladder cuff	-	1.0 cm	3	+	+
			Noninvasive high-grade papillary urothelial carcinoma	HGN	Bladder cuff	-	0.9 cm	4	+	+
			Noninvasive high-grade papillary urothelial carcinoma	HGN	Bladder cuff	-	0.3 cm	5	-	+
4	F/75	pT3pN1pMx	High-grade urothelial carcinoma and small cell carcinoma	HGI	Mid ureter	Periureteric adipose tissue	2.0 cm	6	+	+
			High-grade urothelial carcinoma and small cell carcinoma	HGI	Mid ureter	Periureteric adipose tissue	1.0 cm	7	+	+
5	F/87	pT3NxMx	Invasive high-grade papillary urothelial carcinoma	HGI	Renal pelvis	Renal cortex	4.5 cm	8	+	+
			Invasive high-grade papillary urothelial carcinoma	HGI	Calyces	Sinus fat	0.9 cm	9	+	+
6	M/71	n/a	Ureteritis cystica, no tumor	n/a	-	-	-	10	-	-
			Ureteritis cystica, no tumor	n/a	-	-	-	11	-	-
			Ureteritis cystica, no tumor	n/a	-	-	-	12	-	-
			Ureteritis cystica, no tumor	n/a	-	-	-	13	-	-
			Ureteritis cystica, no tumor	n/a	-	-	-	14	-	-
			Ureteritis cystica, no tumor	n/a	-	-	-	15	-	-
7	F/61	pT3N0Mx	Invasive high-grade papillary urothelial carcinoma	HGI	Distal ureter	Periureteric adipose tissue	1.9 cm	16	+	+
8	M/46	mpTaNxMx	Noninvasive low-grade papillary urothelial carcinoma	LGN	Distal ureter	-	0.9 cm	17	+	+
			Noninvasive low-grade papillary urothelial carcinoma	LGN	Distal ureter	-	0.4 cm	18	+	+
			Noninvasive low-grade papillary urothelial carcinoma	LGN	Distal ureter	-	<0.1 cm	19	-	+

Case	Sex/Age (y)	Pathologic Stage	Pathologic Diagnosis	Grade	Location	Depth	Size	Lesion Number	White Light Diagnosis	NIRF Imaging
9	M/82	pTaN0Mx	Noninvasive high-grade papillary urothelial carcinoma	HGN	Mid ureter	-	4.9 cm	20	+	+
			Noninvasive high-grade papillary urothelial carcinoma	HGN	Distal ureter	-	<0.1 cm	21	-	+
			Noninvasive high-grade papillary urothelial carcinoma	HGN	Distal ureter	-	<0.1 cm	22	-	+
10	M/58	pT1N0Mx	Invasive high-grade papillary urothelial carcinoma with squamous differentiation	HGI	Distal ureter	Lamina propria	5.2 cm	23	+	+
11	M/81	pTaNxMx	Noninvasive low-grade papillary urothelial carcinoma	LGN	Mid ureter	-	2.7 cm	24	+	+
12	M/86	pTaNxMx	Noninvasive high-grade papillary urothelial carcinoma	HGN						
			Ureteropelvic junction	-	4.7 cm	25	+	+		

HGI, high-grade invasive; HGN, high-grade noninvasive; n/a, not applicable tumor grade; LGN, low-grade noninvasive.

Mean patient age is 69.

Table 2a.

Operator characteristics for determination of sensitivity and specificity of ICG-Var 3 pHLIP

		Histopathologic Diagnosis	
		Cancer	No Cancer
NIRF ICG-Var3 pHLIP	Signal	19	0
	No signal	0	6

Author Manuscript

Author Manuscript

Author Manuscript

Author Manuscript

Table 2b.

Operator characteristics for determination of sensitivity and specificity of white light examination

		Histopathologic Diagnosis	
		Cancer	No Cancer
White light	Seen	15	0
	Not seen	4	6

Author Manuscript

Author Manuscript

Author Manuscript

Author Manuscript

Table 3.

Results of sensitivity and specificity tests for 2 visualization methods

Measure	NIRF of ICG-Var3 pHLIP	White Light
Sensitivity	1.000	78.947
Specificity	1.000	1.000
Positive predictive value	1.000	1.000
Negative predictive value	1.000	0.600

Author Manuscript

Author Manuscript

Author Manuscript

Author Manuscript